

Shape Dependence in the Formation of Condensed Phases Exhibited by Disubstituted Sucrose Esters

Valérie Molinier,^[a, d] Paul J. J. Kouwer,^[b, e] Juliette Fitremann,^[a, f] Alain Bouchu,^[a, g] Grahame Mackenzie,^[b] Yves Queneau,^{*,[a]} and John W. Goodby^{*,[c]}

Abstract: We report on the self-organizing properties of sucrose esters that are di-(1',6', 1',6, and 6,6')-substituted with aliphatic chains of identical or different chain lengths and levels of saturation. For the materials possessing two saturated aliphatic chains, the compounds exhibited thermotropic lamellar smectic A phases. A remarkable new

phase transition was observed for the di-octadecanoyl homologue in which one smectic A phase transformed into another with a continuous change in

layer spacing, but with a discontinuous change in the correlation length. The incorporation of long *cis*-unsaturated chains led to increased cross-sectional areas of the chains relative to the sucrose head groups and, hence, columnar phases were observed.

Keywords: fatty acids · glycolipids · liquid crystals · phase transitions · sucrose esters

Introduction

Glycolipids are typically found in the outer leaflets of biological membranes, and there is a particularly high incidence of their presence in the membranes of axons and dendrons found in nerve cells.^[1,2] Furthermore, glycolipids have been used in the creation of artificial membranes and have often been used as nonionic surfactants. In these applications, glycolipids have been shown to possess lyotropic and/or thermotropic liquid-crystal properties.^[3] Property–structure analyses indicate that most thermotropic mesogenic variants are smectic A or columnar phases.^[4] Conversely, the addition of water to glycolipids, which causes swelling of the head groups, results in the formation of lamellar, cubic and/or columnar phases as a function of the induced curvature in the packing arrangements of the molecules. Consequently, a higher degree of liquid-crystalline diversity is found in the lyotropic state relative to the thermotropic state. Interestingly, although this richness is found in the lyotropic state, more materials exhibit thermotropic phases than lyotropic phases. Comparison of the number and range of thermotropic materials with those possessing lyotropic phases indicates that glycolipids are not particularly good amphiphiles.

Sucrose fatty-acid esters are nonionic surfactants, displaying good properties in terms of emulsification, mildness, and toxicology, and are used as food or cosmetic emulsifiers.^[5–16] Due to structural complexity (i.e., mixtures with different patterns of substitution and stereochemistry), the physicochemical properties of defined compounds have been stud-

[a] Dr. V. Molinier, Dr. J. Fitremann, Dr. A. Bouchu, Dr. Y. Queneau
Laboratoire de Chimie Organique
UMR 5181 CNRS; Université Lyon 1; INSA
Institut National des Sciences Appliquées de Lyon
Bât. J. Verne, 20 avenue A. Einstein
69621 Villeurbanne Cedex (France)
Fax: (+33)4724-38896
E-mail: yves.queneau@insa-lyon.fr

[b] Dr. P. J. J. Kouwer, Dr. G. Mackenzie
Department of Chemistry, The University of Hull
Cottingham Road, Hull, HU6 7RX (UK)

[c] Prof. J. W. Goodby
Department of Chemistry, The University of York
Heslington, York, YO10 5DD (UK)
Fax: (+44)1904-432-516
E-mail: jwg500@york.ac.uk

[d] Dr. V. Molinier
Current address:
Laboratoire de Chimie Organique et Macromoléculaire
UMR CNRS 8009, École Nationale Supérieure de Chimie de Lille
BP 108, 59652 Villeneuve D'Ascq Cedex (France)

[e] Dr. P. J. J. Kouwer
Current address: Department of Chemistry, MIT
77 Massachusetts Avenue, Cambridge, MA02139-4307 (USA)

[f] Dr. J. Fitremann
Current address: Laboratoire des IMRCP
CNRS UMR 5623, Université Paul Sabatier
Bât. 2R1, 118 Route de Narbonne, 31062 Toulouse Cedex 4 (France)

[g] Dr. A. Bouchu
Current address: Tereos, Service Innovation
rue du Petit Versailles, B.P. 16, 59239 Thumeries (France)

ied less extensively than other kinds of nonionic surfactants, such as polyoxyethylenic surfactants or alkylpolyglucosides. Although the surface activities and other properties for monosubstituted sucrose esters in solution are well documented,^[17–24] the thermotropic liquid-crystal properties for such materials have only recently been investigated in detail. One commercial mixture of sucrose oleate has been studied,^[25] along with the shear-induced phase transitions of sucrose stearate blends.^[26] More recently, a systematic study of the effects of aliphatic chain length and degree of unsaturation on the thermotropic liquid-crystal properties of monosubstituted sucrose fatty-acid esters has been made.^[27]

Amphiphiles with sugars or cyclic and acyclic polyols as polar heads with single, apolar aliphatic chains attached to the head groups tend to display smectic phases.^[3,4,28–30] Thermotropic columnar mesophases with the head groups located towards the interior of the columns have also been obtained by grafting several fatty-acid chains onto the polar head, thereby increasing the volume ratio of fatty-acid chain to polar head group, leading to changes in curvature and, hence, packing constraints of the molecules.^[3,31–33] Columnar mesophases also have been obtained by increasing the volume of the head group relative to the aliphatic region. Thus, head groups containing more than one sugar moiety, but still possessing a single aliphatic chain, tend to form columnar phases in which the aliphatic chains are located towards the interiors of the columns, with head groups towards the exterior. Interestingly, in such molecular architectures that maintain a rodlike shape, which is the case for most alkylpolyglucosides, smectic phases are again observed.^[34–36] As the polar head becomes more bulky, it also adopts a wedge-shaped conformation, as in the case of certain regioisomers of sucrose hydroxyalkylethers and monosubstituted sucrose fatty-acid esters, with the consequence that columnar or cubic mesophases are observed.^[4,27,37]

In this study, we report on the thermotropic liquid-crystalline properties of amphiphilic glycolipids designed with two aliphatic chains attached at the 1',6', 1'6, and 6,6' positions to the sucrose scaffold. This work is motivated by the fact that both *Cord Factor*, the 6,6'-dimycolic ester of α,α -treha-

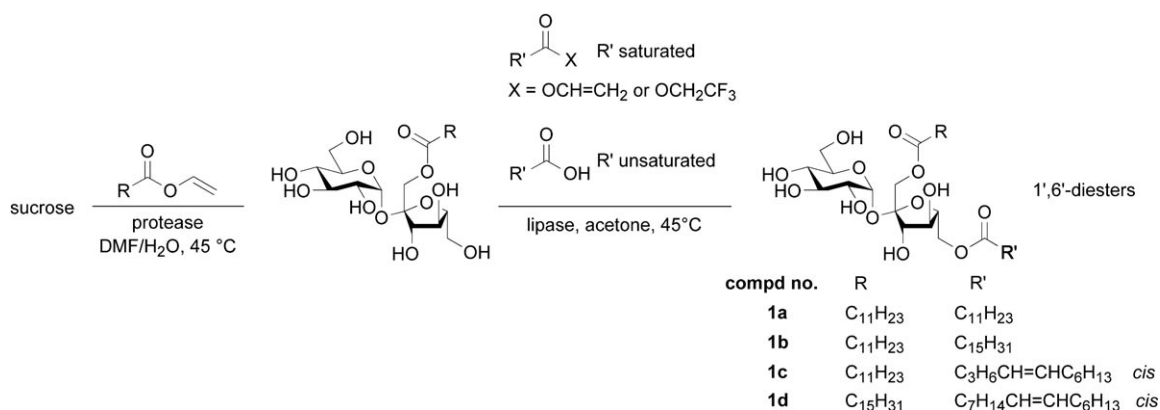
lose, which is associated with virulent strains of *tubercle bacilli*, and 6,6'-di-*O*-palmitoylsucrose possess immunostimulant properties and antitumour activity.^[38–41] Our initial studies on the homologous material, 6,6'-di-*O*-stearoylsucrose, demonstrate that it is liquid crystalline, and forms a smectic liquid-crystal phase in which the molecules have extended conformational structures.^[42] Our results indicate that the liquid-crystal properties of such materials could possibly be important in relation to their biological function. This report provides an extensive study of the self-assembly and self-organization of a broad range of disubstituted sucrose esters.

Compounds **1a–d**, **2a–h**, **3a,b**, and **4a** were synthesized from unprotected sucrose by using selective methods of esterification.^[43] The 1',6'-diesters, **1a–d**, were prepared by enzymatic methods, whereas the 6,6'-diesters **2a–h**, **3a,b**, and the 1',6'-diester, **4a**, were obtained by Mitsunobu coupling reactions.^[44] These methods, though very selective, do not supply totally pure regioisomers, therefore, further purification by using preparative HPLC was required. Due to the known migration phenomena,^[45,46] regioisomers at the secondary positions cannot be synthesized in pure form. Investigations of the thermotropic mesophase behavior and structures of the sucrose derivatives were made by using thermal polarizing light optical microscopy, differential scanning calorimetry, and X-ray diffractometry.

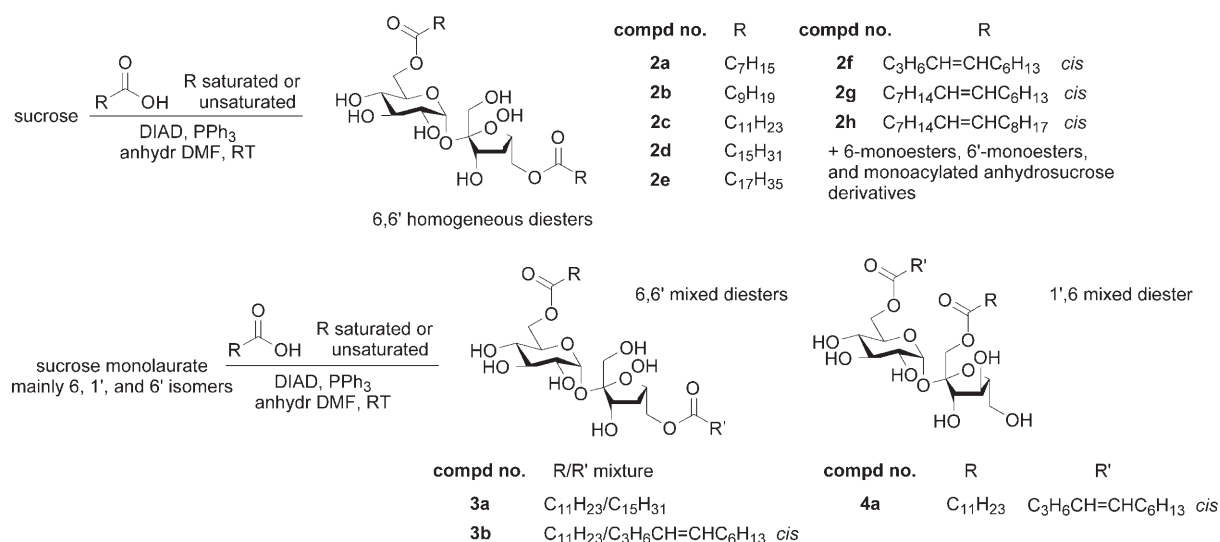
Experimental Section

General synthetic strategies: 1',6'-Diesters **1a–d** were obtained by transesterification of mono-1'-*O*-lauroylsucrose and mono-1'-*O*-palmitoylsucrose with the desired vinyl (or trifluoroethyl) ester (or the corresponding carboxylic acid) in acetone in the presence of a lipase, as described previously.^[47] The starting monoester sample was obtained after a first esterification of unprotected sucrose in the presence of a protease, as described in the literature,^[48–52] and further purification by semipreparative HPLC to obtain the pure 1'-isomer. The synthesis of these 1',6'-diesters is shown in Scheme 1.

Homogeneous 6,6'-diesters **2a–h** were obtained by the reaction of sucrose with the desired carboxylic acid under Mitsunobu conditions (Scheme 2).^[40,41,44] The pure diesters were isolated and purified by semipreparative HPLC. The mixture of diesters comprising **3a**, **3b**, and **4a** was obtained by treatment of sucrose monolaurate under the same condi-



Scheme 1. Synthesis of sucrose 1',6'-diesters by enzymatic methods.



Scheme 2. Synthesis of sucrose, homogeneous, and mixed 6,6'-diesters by the Mitsunobu reaction.

tions. The relative position of the two chains at OH-6 and OH-6', respectively, could not be ascertained for each of the diesters **3a** and **3b**. As these were synthesized from a mixture of monolaurate isomers, they must be considered as a mixture of two compounds.

The purities of the compounds were ascertained by conducting ¹H and ¹³C NMR spectroscopy, HPLC, and HRMS or elemental analysis (if sufficient sample was available).

Evaluation of physical properties: Phase identifications and determination of phase-transition temperatures were carried out, concomitantly, by thermal polarizing light microscopy using a Zeiss Universal polarizing transmitted light microscope equipped with a Mettler FP52 microfurnace in conjunction with an FP50 Central Processor. Photomicrographs were obtained by using a Zeiss polarizing light microscope equipped with a Nikon AFM camera. Differential scanning calorimetry was used to determine enthalpies of transition and to confirm the phase-transition temperatures determined by optical microscopy. Differential scanning thermograms (scan rate 10 °C min⁻¹) were obtained by using a Perkin-Elmer DSC 7 PC system operating on DOS software. The results obtained were standardized to indium (measured onset 156.68 °C, Δ*H* 28.47 J g⁻¹, lit. value 156.60 °C, Δ*H* 28.45 J g⁻¹).^[53]

The X-ray diffraction experiments were performed by using a MAR345 diffractometer equipped with a 2D-image plate detector (CuK_α radiation, graphite monochromator, λ = 1.54 Å). The samples were heated in the presence of a magnetic field (*B* ≈ 1 T) by using a home-built capillary furnace. The diffraction patterns show the intensity as a function of the modulus of the scattering wave vector (*q*). The correlation length was determined by using ORIGIN in conjunction with MARR software. These programmes allow deconvolution of the X-ray peaks and, therefore, determination of the peak width at half the peak height, which can be compared to the peak width of the X-ray beam. The differences were used to determine the correlation length, and the data could then be fitted to a Gaussian or Lorentzian function. Molecular lengths were determined by using either Dreiding molecular models or computer simulations by using an Apple MacIntosh G4 computer and ChemDraw3D as part of a *Chem-Draw Ultra 6.0* program.

Synthetic methods for sucrose diesters

Chemicals: Sucrose was obtained from Béghin-Say. Reactants were purchased from Aldrich and TCI (vinylic esters). Chromatography solvents were purchased from SDS and Carlo Erba. HPLC solvents were purchased from SDS. The enzymes were gifts from Novozyme.

Enzymatically synthesized sucrose 1',6'-diesters 1a-d (Scheme 1): 1',6'-Diesters were synthesized as described,^[47] by transesterification of pure 1'-monoester (obtained as in refs. [48–51]) with the desired trifluoroethyl

or vinylic ester or carboxylic acid in the presence of a lipase. The 1'-monoester (1'-*O*-palmitoylsucrose, 86 mg, 0.15 mmol) was dissolved in acetone (1.5 mL). The acylating agent (palmitoleyl acid trifluoroethyl ester, 254 mg, 5 equiv) was added, followed by the immobilized lipase (Novozyme 435, 170 mg). The reaction was conducted at 45 °C under slow magnetic stirring (100 rpm) for 16 h (up to 40 h in some cases). The 1',6'-diester was obtained after filtration, evaporation of the solvent and purification on a silica-gel column eluted with dichloromethane/acetone/methanol/water 78:10:10:1.5 v/v (*R*_f = 0.25 for compound **1d**, 46 mg, 38 %).

1'-*O*-Lauroyl-6'-*O*-palmitoylsucrose 1b: [*α*]_D = +36 (*c* = 0.6, THF); ¹H NMR (500 MHz, MeOD): δ = 0.83–1.11 (m, 6H; 2CH₃), 1.17–1.47 (m, 40H; (CH₂)₂₀), 1.56–1.73 (m, 4H; 2CH₂), 2.28–2.45 (m, 4H; 2CH₂), 3.36 (t + MeOD, 1H; *J*_{4,5} = *J*_{5,6} = 9.5 Hz, H₄), 3.42 (dd, 1H; *J*_{2,3} = 9.5 Hz, *J*_{2,1} = 3.8 Hz, H₂), 3.69 (t, 1H; *J*_{3,4} = *J*_{3,2} = 9.5 Hz, H₃), 3.73 (dd, 1H; *J*_{6b,6a} = 12.3 Hz, *J*_{6b,5} = 5.4 Hz, H_{6b}), 3.80–3.87 (m, 2H; H_{6a}, H₅), 3.88 (td, 1H; *J*_{5,4} = *J*_{5,6a} = 8.3 Hz, *J*_{5,6b} = 2.8 Hz, H₅), 4.03 (t, 1H; *J*_{4,3'} = *J*_{4,5'} = 8.3 Hz, H₄), 4.08 (d, 1H; *J*_{3,4'} = 8.3 Hz, H₃), 4.12 (d, 1H; *J*_{1b,1'a} = 12.0 Hz, H_{1b}), 4.33 (dd, 1H; *J*_{6b,6'a} = 11.8 Hz, *J*_{6b,5'} = 2.8 Hz, H_{6b}), 4.39 (d, 1H; *J*_{1'a,1'b} = 12.0 Hz, H_{1'a}), 4.40 (dd, 1H; *J*_{6'a,6'b} = 11.8 Hz, *J*_{6'a,5'} = 8.0 Hz, H_{6'a}), 5.36 ppm (d, 1H; *J*_{1,2} = 3.8 Hz, H₁); ¹³C NMR (125 MHz, MeOD): δ = 14.7 (2CH₃), 26.3, 26.4 (2CH₂), 24.0, 30.5, 30.7, 30.8, 30.9, 31.0, 31.1, 33.4, 33.4 (20CH₂), 35.3 (2CH_{2a}), 62.8 (C₆), 63.8 (C₁), 67.0 (C₆), 71.8 (C₄), 73.4 (C₂), 74.6 (C₅), 75.0 (C₃), 76.4 (C₄), 78.7 (C₃), 81.1 (C₅), 94.3 (C₁), 104.6 (C₂), 174.9 (1C=O on 1'), 175.7 ppm (1C=O on 1'); HRMS: *m/z*: calcd for C₄₀H₇₄O₁₃Na: 785.5027; found: 785.5040 [*M*+Na]⁺; elemental analysis calcd (%) for C₄₀H₇₄O₁₃·1.9H₂O: C 60.26, H 9.84; found: C 60.21, H 9.43.

1'-*O*-Lauroyl-6'-*O*-dodec-5c-enoilsucrose 1c: [*α*]_D = +35 (*c* = 0.3, THF); ¹H NMR (500 MHz, MeOD): δ = 0.88–0.98 (m, 6H; 2CH₃), 1.23–1.43 (m, 24H; (CH₂)₁₂), 1.61–1.74 (m, 4H; 2CH₂), 2.01–2.16 (m, 4H; CH₂CH=CHCH₂), 2.34–2.43 (m, 4H; 2CH_{2a}), 3.36 (t + MeOD, 1H; *J*_{4,3} = *J*_{4,5} = 9.7 Hz, H₄), 3.42 (dd, 1H; *J*_{2,3} = 9.7 Hz, *J*_{2,1} = 3.9 Hz, H₂), 3.69 (t, 1H; *J*_{3,4} = *J*_{3,2} = 9.7 Hz, H₃), 3.73 (dd, 1H; *J*_{6b,6a} = 11.7 Hz, *J*_{6b,5} = 4.7 Hz, H_{6b}), 3.80–3.87 (m, 2H; H_{6a}, H₅), 3.90 (td, 1H; *J*_{5,4} = *J*_{5,6'a} = 8.0 Hz, *J*_{5,6'b} = 3.0 Hz, H₅), 4.03 (t, 1H; *J*_{4,3'} = *J*_{4,5'} = 8.0 Hz, H₄), 4.08 (d, 1H; *J*_{3,4'} = 8.0 Hz, H₃), 4.12 (d, 1H; *J*_{1b,1'a} = 12.0 Hz, H_{1b}), 4.33 (dd, 1H; *J*_{6b,6'a} = 11.8 Hz, *J*_{6b,5'} = 3.0 Hz, H_{6b}), 4.39 (d, 1H; *J*_{1'a,1'b} = 12.0 Hz, H_{1'a}), 4.41 (dd, 1H; *J*_{6'a,6'b} = 11.8 Hz, *J*_{6'a,5'} = 8.0 Hz, H_{6'a}), 5.31, 5.48 ppm (m, 3H; H₁, CH=CH); ¹³C NMR (125 MHz, MeOD): δ = 14.8 (2CH₃), 26.3, 26.4 (2CH₂), 27.8, 28.5 (2CH_{2a}CH=CH), 24.0, 30.4, 30.5, 30.8, 30.8, 31.0, 31.1, 31.1, 33.3, 33.4 (12CH₂), 34.6, 35.3 (2CH_{2a}), 62.7 (C₆), 63.7 (C₁), 67.0 (C₆), 71.8 (C₄), 73.3 (C₂), 74.6 (C₅), 74.9 (C₃), 76.3 (C₄), 78.6 (C₃), 81.1 (C₅), 94.3 (C₁), 104.5 (C₂), 129.9, 132.3 (CH=CH), 174.9 (1C=O on 1'),

175.6 ppm (1C=O on 6'); HRMS: m/z : calcd for $C_{36}H_{64}O_{13}Li$: 711.4507; found: 711.4509 $[M+Li]^+$.

1'-O-Palmitoyl-6'-O-hexadec-9-c-enoilsucrose 1d: $[\alpha]_D = +17$ ($c = 0.6$, THF); 1H NMR (500 MHz, MeOD): $\delta = 0.85\text{--}0.98$ (m, 6H; 2CH₃), 1.14–1.50 (m, 40H; (CH₂)₂₀), 1.57–1.73 (m, 4H; 2CH_{2p}), 2.12–2.98 (m, 4H; CH₂CH=CHCH₂), 2.29–2.45 (m, 4H; 2CH_{2a}), 3.36 (dd + MeOD, 1H; $J_{4,3} = 9.1$ Hz, $J_{4,5} = 9.8$ Hz, H₄), 3.42 (dd, 1H; $J_{2,3} = 9.7$ Hz, $J_{2,1} = 3.8$ Hz, H₂), 3.69 (dd, 1H; $J_{3,4} = 9.1$ Hz, $J_{3,2} = 9.7$ Hz, H₃), 3.73 (dd, 1H; $J_{6b,6a} = 12.0$ Hz, $J_{6b,5} = 5.0$ Hz, H_{6b}), 3.80–3.87 (m, 2H; H_{6a}, H₅), 3.90 (td, 1H; $J_{5,4} = J_{5,6a} = 8.2$ Hz, $J_{5,6b} = 3.2$ Hz, H₅), 4.03 (t, 1H; $J_{4,3} = J_{4,5} = 8.2$ Hz, H₄), 4.08 (d, 1H; $J_{3,4} = 8.2$ Hz, H₃), 4.12 (d, 1H; $J_{1b,1a} = 12.3$ Hz, H_{1b}), 4.33 (dd, 1H; $J_{6b,6a} = 11.8$ Hz, $J_{6b,5} = 3.2$ Hz, H_{6b}), 4.39 (d, 1H; $J_{1a,1b} = 12.3$ Hz, H_{1a}), 4.41 (dd, 1H; $J_{6a,6b} = 11.8$ Hz, $J_{6a,5} = 8.2$ Hz, H_{6a}), 5.31–5.44 ppm (m, 3H; H₁, CH=CH); ^{13}C NMR (125 MHz, MeOD): $\delta = 14.8$ (2CH₃), 26.3, 26.4 (2CH_{2p}), 28.4, 28.5 (2CH_{2a}CH=CH), 24.0, 30.4, 30.5, 30.6, 30.8, 31.0, 31.1, 33.2, 33.4 (20CH₂), 35.3, 35.3 (2CH_{2a}), 62.8 (C₆), 63.7 (C₁), 67.0 (C₆), 71.8 (C₄), 73.4 (C₂), 74.6 (C₅), 74.9 (C₃), 76.4 (C₄), 78.7 (C₃), 81.1 (C₅), 94.3 (C₁), 104.6 (C₂), 131.1, 131.2 (CH=CH), 174.9 (1C=O on 1'), 175.7 ppm (1C=O on 6'); HRMS: m/z : calcd for $C_{44}H_{80}O_{13}Li$: 823.5759; found: 823.5766 $[M+Li]^+$.

Sucrose 6,6'-diesters 2a–h, 3a,b, and 4a synthesized through the Mitsunobu reaction (Scheme 2)^[44]

Homogeneous 6,6'-diesters 2a–h

Sucrose (3.42 g, 10.0 mmol) was dissolved in anhydrous DMF (79 mL) by stirring under N₂ at 70°C. The mixture was cooled to RT before addition of triphenylphosphine (7.06 g, 2.7 equiv), carboxylic acid (lauric acid, 5.00 g, 2.5 equiv), and more DMF (21 mL). After complete dissolution, the medium was cooled to 0°C and diisopropyl azodicarboxylate (DIAD) (5.3 mL, 2.7 equiv) was added. TLC showed nearly total consumption of sucrose after 26 h at RT. After removal of DMF under reduced pressure at $T = 36\text{--}38^\circ\text{C}$, the crude residue was subjected to chromatography on a silica-gel column (elution gradient: dichloromethane/acetone/methanol/water 78:10:10:1.5–67:15:15:3 v/v). The diester fraction (containing anhydroderivatives as side products) was collected (1.30 g, 18%) and subjected further to semipreparative HPLC on a NH₂ Spherisorb column, 20×250 mm (injection loop: 2 mL, flow: 20 mL min⁻¹), by using a CH₃CN/THF/water 40:54:6 v/v mixture, leading to pure 6,6'-diester (6,6'-di-*O*-lauroyl sucrose, 15%).

6,6'-Di-*O*-lauroylsucrose 2c: $[\alpha]_D = +45$ ($c = 1$, THF); ref. [47]; 1H NMR (300 MHz, MeOD): $\delta = 0.80\text{--}1.00$ (m, 6H; 2CH₃), 1.15–1.45 (m, 32H; 2(CH₂)₈), 1.50–1.70 (m, 4H; 2CH_{2p}), 2.25–2.45 (m, 4H; 2CH_{2a}), 3.23 (t, 1H; $J_{4,3} = J_{4,5} = 9.4$ Hz, H₄), 3.41 (dd, 1H; $J_{2,3} = 9.4$ Hz, $J_{2,1} = 3.7$ Hz, H₂), 3.56 (d, 1H; $J_{1b,1a} = 12.8$ Hz, H_{1b}), 3.62 (d, 1H; $J_{1a,1b} = 12.8$ Hz, H_{1a}), 3.70 (t, 1H; $J_{3,4} = J_{3,2} = 9.4$ Hz, H₃), 3.86–4.15 (m, 5H; H_{6b}, H₃, H₅, H₄, H₅), 4.30–4.40 (m, 2H; H_{6a/b}), 4.44 (dd, 1H; $J_{6a,6b} = 10.9$ Hz, $J_{6a,5} \sim 0$, H_{6a}), 5.33 ppm (d, 1H; $J_{1,2} = 3.7$ Hz, H₁); ^{13}C NMR (75 MHz, MeOD): $\delta = 14.8$ (2CH₃), 26.3 (2CH_{2p}), 24.1, 30.5, 30.8, 31.0, 31.1, 33.4 (16CH₂), 35.2 (2CH_{2a}), 64.3 (C₁), 65.5 (C₆), 67.2 (C₆), 72.2 (C₅, C₄), 73.5 (C₂), 74.9 (C₃), 77.1 (C₄), 79.2 (C₃), 81.0 (C₅), 93.5 (C₁), 105.6 (C₂), 175.4 (1C=O on 6'), 175.8 ppm (1C=O on 6'); HRMS: m/z : calcd for $C_{36}H_{66}O_{13}Na$: 729.4401; found: 729.4400 $[M+Na]^+$; elemental analysis calcd (%) for $C_{36}H_{66}O_{13}$: C 61.17, H 9.41, O 29.42; found: C 61.16, H 9.31, O 28.96.

6,6'-Di-*O*-stearoylsucrose 2e: $[\alpha]_D = +39$ ($c = 0.4$, THF); 1H NMR (300 MHz, CDCl₃/MeOD 2/1): $\delta = 0.89$ (m, 6H; 2CH₃), 1.28 (m, 56H; 2(CH₂)₁₄), 1.62 (m, 4H; 2CH_{2p}), 2.35 (m, 4H; 2CH_{2a}), 3.27 (t + MeOD, 1H; $J_{4,3} = J_{4,5} = 9.4$ Hz, H₄), 3.46 (dd, 1H; $J_{2,1} = 3.7$ Hz, $J_{2,3} = 10.0$ Hz, H₂), 3.59 (d, 1H; $J_{1b,1a} = 12.2$ Hz, H_{1b}), 3.66 (d, 1H; $J_{1a,1b} = 12.6$ Hz, H_{1a}), 3.72 (t, 1H; $J_{3,4} = J_{3,2} = 9.3$ Hz, H₃), 3.88–4.10 (m, 4H; H₅; t, $J_{4,3} = J_{4,5} = 7.6$ Hz, H₄, H₅, H₅), 4.15 (dd, 1H; $J_{6b,6a} = 11.8$ Hz, $J_{6b,5} = 6.1$ Hz, H_{6b}), 4.36 (m, 2H; H_{6a/b}), 4.44 (dd, 1H; $J_{6a,6b} = 11.3$ Hz, $J_{6a,5} < 1$, H_{6a}), 5.36 ppm (d, 1H; $J_{1,2} = 3.8$ Hz, H₁); ^{13}C NMR (75 MHz, MeOD/CDCl₃ (4:1 v/v) at 50°C): $\delta = 14.4$ (2CH₃), 25.4 (2CH_{2p}), 23.2, 29.7, 29.8, 30.0, 30.2, 32.4 (28CH₂), 34.6, 34.7 (2CH_{2a}), 64.4 (C₁), 64.5 (C₆), 66.2 (C₆), 71.1 (C₄), 71.4 (C₃), 72.4 (C₂), 74.2 (C₃), 76.8 (C₄), 80.1 (C₃), 80.3 (C₅), 92.5 (C₁), 104.7 (C₂), 174.7 (1C=O on 6'), 175.1 ppm (1C=O on 6'); HRMS: m/z : calcd for $C_{48}H_{90}O_{13}Na$: 897.6279; found: 897.6271 $[M+Na]^+$; elemental analysis calcd (%) for $C_{48}H_{90}O_{13}$: C 65.87, H 10.36, O 23.76; found: C 65.51, H 10.51, O 23.26.

Mixtures of 6,6'- and 1',6'-diesters 3a, 3b, and 4a

Monolauroyl sucrose (mixture of isomers, 6/1/6': 40:10:33, 1.00 g, 1.9 mmol) was dissolved in anhydrous DMF (20 mL) under N₂ at RT. Triphenylphosphine (1.26 g, 2.5 equiv) and carboxylic acid (dodec-5-*c*-enoic acid, 0.84 mL, 2 equiv) were added. After complete dissolution, the medium was cooled to 0°C and DIAD (0.94 mL, 2.5 equiv) was added. TLC showed the formation of less-polar products without total consumption of monolauroyl sucrose. After 17 h at RT, DMF was removed under reduced pressure at $T = 36\text{--}38^\circ\text{C}$ and the crude residue was subjected to chromatography on a silica-gel column (elution gradient: dichloromethane/acetone/methanol/water 78:10:10:1.5–67:15:15:3 v/v). The main mixed diester was collected ($R_f = 0.49$ in the 67:15:15:3 v/v eluent, the mixed 6,6'-diester, 453 mg, 34%) together with a second mixed diester ($R_f = 0.60$ in the 67:15:15:3 v/v eluent, 1'-*O*-dodec-5-*c*-enoyl-6-*O*-lauroyl sucrose, 94 mg, 7%). These were subjected further to semipreparative HPLC on a NH₂ spherisorb column, 20×250 mm (injection loop: 2 mL, flow: 20 mL min⁻¹) by using a CH₃CN/THF/water 40:54:6 v/v eluent to give the pure mixed diesters.

In the mixed 6,6'-diester, the relative positions of the chains on OH-6 and OH-6' could not be ascertained, thus, **3a** and **3b** should be considered as mixtures of compounds (**3a** = 6C₁₂-6'C₁₆ + 6C₁₆-6'C₁₂ and **3b** = 6C₁₂-6'C_{12,1} + 6C_{12,1}-6'C₁₂).

6-*O*-Palmitoyl-6'-*O*-lauroylsucrose and 6-*O*-lauroyl-6'-*O*-palmitoylsucrose 3a: $[\alpha]_D = +41$ ($c = 1$, THF); 1H NMR (300 MHz, MeOD/CDCl₃ 25:75): $\delta = 0.77\text{--}0.95$ (m, 6H; 2CH₃), 1.15–1.40 (m, 40H; (CH₂)₂₀), 1.50–1.75 (m, 4H; 2CH_{2p}), 2.25–2.43 (m, 4H; 2CH_{2a}), 3.26 (dd, 1H; $J_{4,3} = 9.0$ Hz, $J_{4,5} = 10.0$ Hz, H₄), 3.46 (dd, 1H; $J_{2,3} = 9.6$ Hz, $J_{2,1} = 3.7$ Hz, H₂), 3.57 (d, 1H; $J_{1b,1a} = 12.4$ Hz, H_{1b}), 3.66 (d, 1H; $J_{1a,1b} = 12.4$ Hz, H_{1a}), 3.76 (dd, 1H; $J_{3,4} = 9.0$ Hz, $J_{3,2} = 9.6$ Hz, H₃), 3.88–4.08 (m, 4H; H₅, H₃, H₄, H₅), 4.17 (dd, 1H; $J_{6b,6a} = 11.8$ Hz, $J_{6b,5} = 5.9$ Hz, H_{6b}), 4.23–4.45 (m, 3H; H_{6a}, H_{6a/b}), 5.36 ppm (d, 1H; $J_{1,2} = 3.7$ Hz, H₁); ^{13}C NMR (75 MHz, MeOD): $\delta = 14.6$ (2CH₃), 25.6 (2CH_{2p}), 23.4, 29.9, 30.1, 30.3, 30.4, 32.7 (20CH₂), 34.7, 34.8 (2CH_{2a}), 64.3 (C₁), 64.7 (C₆), 66.6 (C₆), 71.2 (C₄), 71.4 (C₃), 72.6 (C₂), 74.1 (C₃), 76.6 (C₄), 79.7 (C₃), 80.3 (C₅), 92.6 (C₁), 104.6 (C₂), 175.0 (1C=O on 6'), 175.4 ppm (1C=O on 6'); HRMS: m/z : calcd for $C_{40}H_{74}O_{13}Na$: 785.5027; found: 785.5023 $[M+Na]^+$; elemental analysis calcd (%) for $C_{40}H_{74}O_{13}$: C 61.94, H 9.80, O 28.26; found: C 61.88, H 9.79, O 28.06.

6-*O*-Dodec-5-*c*-enoyl-6'-*O*-lauroylsucrose and 6-*O*-lauroyl-6'-*O*-dodec-5-*c*-enoylsucrose 3b: $[\alpha]_D = +44$ ($c = 6$, THF); 1H NMR (500 MHz, MeOD): $\delta = 0.88\text{--}0.97$ (m, 6H; 2CH₃), 1.25–1.42 (m, 24H; (CH₂)₁₂), 1.58–1.75 (m, 4H; 2CH_{2p}), 2.01–2.16 (m, 4H; CH₂CH=CHCH₂), 2.32–2.49 (m, 4H; 2CH_{2a}), 3.27 (dd, 1H; $J_{4,3} = 9.1$ Hz, $J_{4,5} = 9.8$ Hz, H₄), 3.45 (dd, 1H; $J_{2,3} = 9.5$ Hz, $J_{2,1} = 3.9$ Hz, H₂), 3.61 (d, 1H; $J_{1b,1a} = 12.3$ Hz, H_{1b}), 3.65 (d, 1H; $J_{1a,1b} = 12.3$ Hz, H_{1a}), 3.74 (dd, 1H; $J_{3,4} = 9.1$ Hz, $J_{3,2} = 9.5$ Hz, H₃), 3.98–3.92 (m, 1H; H₅), 4.03 (t, 1H; $J_{4,3} = J_{4,5} = 8.2$ Hz, H₄), 4.16–4.05 (m, 3H; H_{6b}, H₃, H₅), 4.42–4.35 (m, 2H; H_{6a/b}), 4.47 (dd, 1H; $J_{6a,6b} = 11.7$ Hz, $J_{6a,5} = 1.6$ Hz, H_{6a}), 5.39 ppm (m, 3H; H₁, CH=CH); ^{13}C NMR (125 MHz, MeOD): $\delta = 14.8$ (2CH₃), 26.3 (2CH_{2p}), 28.5, 27.8 (2CH_{2a}CH=CH), 24.0, 30.4, 30.5, 30.8, 30.9, 31.0, 31.1, 33.2, 33.4 (12CH₂), 34.6, 35.2 (2CH_{2a}), 64.3 (C₁), 65.5 (C₆), 67.2 (C₆), 72.1 (C₅, C₄), 73.4 (C₂), 74.8 (C₃), 77.1 (C₄), 79.2 (C₃), 81.0 (C₅), 93.4 (C₁), 105.6 (C₂), 130.0, 131.2 (CH=CH), 175.4 (1C=O on 6'), 175.6 ppm (1C=O on 6'); HRMS: m/z : calcd for $C_{30}H_{54}O_{11}Na$: 727.4245; found: 727.4248 $[M+Na]^+$; elemental analysis calcd (%) for $C_{36}H_{64}O_{13}$: C 59.96, H 9.20; found: C 59.95, H 9.13.

1'-*O*-Dodec-5-*c*-enoyl-6-*O*-lauroylsucrose 4a: $[\alpha]_D = +31$ ($c = 0.4$, THF); 1H NMR (500 MHz, MeOD): $\delta = 0.80\text{--}1.00$ (m, 6H; 2CH₃), 1.20–1.50 (m, 24H; (CH₂)₁₂), 1.55–1.75 (m, 4H; 2CH_{2p}), 2.00–2.20 (m, 4H; CH₂CH=CHCH₂), 2.30–2.50 (m, 4H; 2CH_{2a}), 3.31 (dd + MeOD, 1H; $J_{4,3} = 9.4$ Hz, $J_{4,5}$ nd, H₄), 3.42 (dd, 1H; $J_{2,3} = 9.8$ Hz, $J_{2,1} = 3.8$ Hz, H₂), 3.68 (dd, 1H; $J_{3,4} = 9.4$ Hz, $J_{3,2} = 9.8$ Hz, H₃), 3.73–3.85 (m, 3H; H_{6a/b}, H₅), 4.00–4.08 (m, 2H; H₅, H₄), 4.09 (d, 1H; $J_{3,4} = 8.5$ Hz, H₃), 4.14 (d, 1H; $J_{1b,1a} = 12.0$ Hz, H_{1b}), 4.19 (dd, 1H; $J_{6b,6a} = 11.8$ Hz, $J_{6b,5} = 5.5$ Hz, H_{6b}), 4.38 (d, 1H; $J_{1a,1b} = 12.0$ Hz, H_{1a}), 4.43 (dd, 1H; $J_{6a,6b} = 11.8$ Hz, $J_{6a,5} = 1.9$ Hz, H_{6a}), 5.41 ppm (m, 3H; H₁, CH=CH); ^{13}C NMR (125 MHz, MeOD): $\delta = 14.7$ (2CH₃), 26.3 (2CH_{2p}), 27.8, 28.5 (2CH_{2a}CH=CH), 24.0, 30.4, 30.5, 30.7, 30.8, 30.9, 31.0, 31.1, 33.3, 33.4 (12CH₂), 34.6, 35.3 (2CH_{2a}), 64.0 (C₁, C₆), 65.0 (C₆), 72.0 (C₄), 72.3 (C₅), 73.3 (C₂), 74.7 (C₃), 75.6 (C₄), 79.0

(C₃), 84.3 (C₅), 94.3 (C₁), 104.4 (C₂), 129.9, 132.3 (CH=CH), 175.0 (1C=O on 1'), 175.7 ppm (1C=O on 6); HRMS: *m/z*: calcd for C₃₀H₅₄O₁₁Na: 727.4245; found: 727.4245 [M+Na]⁺.

Results and Discussion

The results are detailed in two sections, depending on the incorporation or not of unsaturations in the aliphatic chains. In Section 1, we describe the thermotropic behavior and the structural features of the saturated fatty-acid derivatives, and in particular we examine the nature of the clearing points and the packing of the molecules in the lamellar phases.

1. Saturated fatty-acid diesters

Classification of the mesophases formed by the compounds **1a**, **1b**, **2a–2e**, and **3a** by optical microscopy, differential scanning calorimetry (DSC), and X-ray diffraction:

Polarizing optical microscopy (POM): Table 1 summarizes the transition temperatures, determined on heating, for the saturated diesters. The lengths and positions of attachment of the aliphatic chains markedly affect the transition temperatures. For example, compare the transition temperatures of compounds **1a** and **2c**. There is approximately a 50 °C difference in the clearing points, possibly because **2c** has a more linear structure than **1a**. Thus, the relative stereochemistries of the materials appear to be important with respect to mesophase thermal stability.

Examination of the microscopic defect textures of the materials showed that all of the compounds exhibited lamellar smectic A phases (see, for example, Figure 1). Under crossed polars (x100), and upon cooling from the isotropic liquid, the mesophases separated in the form of *bâtonnets*

that coalesced to form various defect patterns. Typically focal-conic defects possessing elliptical and hyperbolic optical discontinuities were formed, together with homeotropic textures. Oily streaks associated with edge dislocations were also observed, and fanlike defect fringes were found to form around air bubbles. These features are diagnostic for the presence of the smectic A phase, and are indicated by the white arrows in Figure 1a. Furthermore, the presence of homeotropic defect textures (Figure 1b) unequivocally demonstrates that there are no tilted smectic phases present for these materials.



Figure 1. Defect textures of the smectic A phase of 6,6'-di-O-octanoylsucrose, **2a**, (x100); a) the oily streak texture and fanlike defects around air bubbles, b) the focal-conic defect and homeotropic textures.

Table 1. Transition temperatures of the saturated fatty-acid sucrose diesters determined by thermal polarizing light microscopy as a function of aliphatic chain lengths.

Compound structure	Chain length	Compound	Transition temperature [°C]
 1',6'-diesters	$m = n = 10$	1a	cryst. 42.1 smectic A 120 iso. liq.
	$m = 10, n = 14$	1b	cryst. ~30 smectic A 115.9 iso. liq.
 6,6'-diesters	$m = n = 6$	2a	soft solid-smectic A 146.3 iso. liq. ^[a]
	$m = n = 8$	2b	cryst. ~90 smectic A 163.0 iso. liq.
	$m = n = 10$	2c	cryst. 87.3 smectic A 170.8 iso. liq.
	$m = n = 14$	2d	cryst. 106.6 smectic A 167.8 iso. liq.
	$m = n = 16$	2e	cryst. 109.7 smectic A 164.3 iso. liq.
	$m = 10, n = 14 +$ $m = 14, n = 10$	3a	cryst. 84.7 smectic A 167.8 iso. liq.

[a] The melting point could not be determined by microscopy or DSC.

If the clearing-point temperatures for the **2a–e** family of compounds are evaluated as a function of chain length, it can be shown that the liquid-crystal mesophase is stabilized as the two aliphatic chains are lengthened up to the dodecanoyl homologues. This behavior is typical of most glycolipids; however, as the chain length is increased further, there is a drop in the clearing points followed by a further rise in temperature. The drop cannot be attributed to impurities associated with the dihexadecanoyl homologue, as the materials in the series have similar purity levels, and

the transitions from the liquid crystal to the liquid states are sharp in all cases. The details in respect of the depression in the clearing points as a function of chain length were investigated further by X-ray diffraction, the results for which will be described in the subsequent Section.

Notably, the classification of the mesophase is smectic A, however, as the materials are chiral, the environmental symmetry of the phase is reduced from D_{8h} to D_8 , and as a consequence, the mesophase should exhibit electroclinic properties. Thus, by symmetry, the mesophases should be classified as SmA^* .

Differential scanning calorimetry (DSC): Results of DSC confirmed the transition temperatures obtained from polarizing light microscopy. Table 2 lists the enthalpy and entropy

Table 2. Enthalpies, ΔH , and entropies, ΔS , for the clearing-point transitions of the saturated fatty-acid esters.

Compd	ΔH [J g ⁻¹]	ΔS [mJ g ⁻¹ K ⁻¹]	Compd	ΔH [J g ⁻¹]	ΔS [mJ g ⁻¹ K ⁻¹]
2a	5.731	13.7	2d	1.633	3.7
2b	4.373	10.0	2e	1.147	2.6
2c	3.07	6.9	3a	1.972	4.5

values as a function of chain length for the 6,6'-esters. A progressive decrease in the enthalpies for the clearing points was a function of increasing saturated fatty-acid chain length. A similar change in the entropy for this transition shows that the smectic A phase becomes more disordered and liquidlike as the fatty-acid chain increases in length. The rate of decrease in the enthalpy and entropy as a function of chain length, per methylene unit, appears to be linear up to the dodecanoyl homologue ($m=n=10$), at which point the rate of change falls off more sharply.

X-ray diffraction studies: X-ray diffraction studies were performed on compounds **1b**, **2a**, **2d**, **2e**, and **3a** over a wide temperature range in the liquid-crystal phase. The results obtained for selected members **2a**, **2d**, and **2e** are described first.

6,6'-Di-O-octanoylsucrose (2a): Figure 2 shows the diffraction intensity for **2a** as a function of scattering vector, q , and temperature. The diffraction data taken at a temperature of 50 °C are summarized in Table 3, and show that the mesophase formed is a lamellar smectic phase. The (001) reflection gives a layer spacing of 28.1 Å, which is similar to the calculated molecular length of 28.2 Å. Coupling this result with those from optical microscopy confirms that the mesophase is smectic A with the molecules arranged orthogonal to the layer planes. Interestingly, the presence of the fourth-order reflection indicates that the layers are relatively well defined, rather than diffuse. Apart from the (001) reflection, all of the other reflections are relatively weak, with the (003) reflection being slightly weaker than the (004). In addition, although the (002) reflection is seen over the tem-

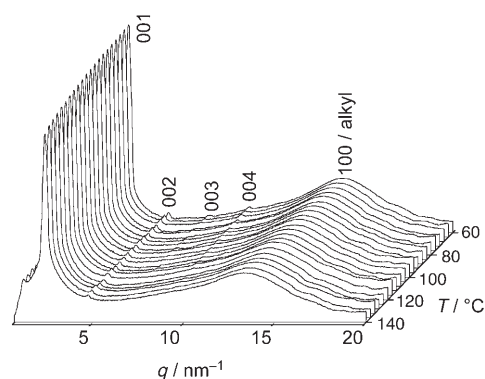


Figure 2. Radially integrated diffraction pattern of 6,6'-di-O-octanoylsucrose, **2a**, over a temperature range of 30–60 °C. Diffraction intensities are given on a logarithmic scale.

Table 3. Distances (d) related to the Miller indices for the radially integrated diffraction pattern of 6,6'-di-O-octanoylsucrose, **2a**, at 50 °C.

Miller index	q [nm ⁻¹]	d [Å]	Ratio
001	2.20	28.6	1
002	4.39	14.3	1/2
003	6.63	9.5	1/3
004	8.82 ^[a]	7.1	1/4
alkyl	13.9	4.5	–

[a] Weak reflection.

perature range of the mesophase, the (003) and (004) reflections occur at lower temperatures, indicating that the layers become better defined as the temperature is lowered.

The temperature dependence of the layer spacing d_{001} and the correlation length ξ_{001} are presented together in Figure 3. A large, but characteristic, temperature dependence of the layer spacing is observed, that is, a nearly

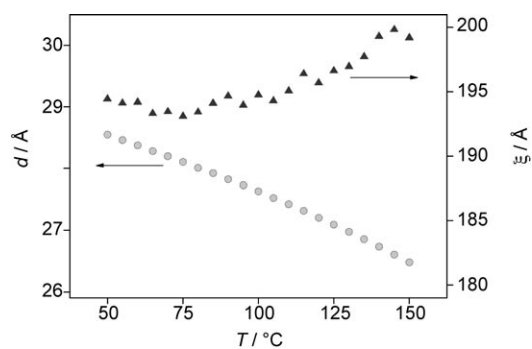


Figure 3. Temperature dependence of d_{001} and ξ_{001} for 6,6'-di-O-octanoylsucrose, **2a**.

linear increase in the layer spacing of approximately 2 Å was observed over a 100 °C temperature range (~7.5% change). Conversely, the correlation length remained relatively constant over the same temperature range.

6,6'-Di-O-hexadecanoylsucrose (2d): Figure 4 shows the diffraction intensity as a function of q and the temperature for

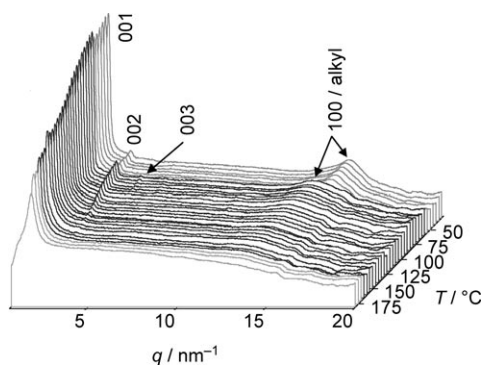


Figure 4. Radially integrated diffraction pattern of 6,6'-di-*O*-hexadecanoylsucrose, **2d**, over a temperature range of 30–180 °C. Diffraction intensities are given on a logarithmic scale.

compound **2d**. The wide-angle reflection is very diffuse throughout the temperature range of the smectic phase and only becomes sharper in the crystal phase. The (001) value of 44.9 Å at 50 °C (the lowest temperature at which the smectic phase can exist) is slightly shorter than the calculated molecular length of 49.7 Å, and, thus, with the observations made by polarizing light microscopy, the phase is confirmed as smectic A. A (002) reflection is visible upon cooling from 145 °C, and a very weak (003) reflection is observed at temperatures below 80 °C. There is an indication that a (004) reflection is present, but it is very weak and is lost partly in the noise. Thus, the layers for **2d** are much less well defined than those for **2a**. This suggests that the longer hexadecyl chains in **2d** are having a disordering effect due to their increased flexibility relative to the octyl chain of **2a**. The diffraction data at 50 °C are summarized in Table 4. The compiled data as a function of temperature are shown in Figure 5.

Table 4. Distances (d) related to the Miller indices for the radially integrated diffraction pattern of 6,6'-di-*O*-hexadecanoylsucrose, **2d**, at 50 °C.

Miller index	q [nm ⁻¹]	d [Å]	Ratio
001	1.40	44.9	1
002	2.78	22.6	1/2
003	4.19	15.0	1/3
alkyl	13.6	4.6	–

The temperature dependence of the layer spacing d_{001} and the correlation length ξ_{001} are shown together in Figure 5. A strong temperature dependence of the layer spacing is observed for the smectic phase, with the d values ranging from 35 to 45 Å. Thus, over a temperature range of 125 °C the layer spacing of the smectic A varies by approximately 20–25%; therefore, the behavior of this smectic A phase is very different from the smectic A phase of compound **2a**. Crystallization is observed between 50 and 60 °C, at which d_{001} and ξ_{001} become virtually temperature independent. At the transition from the smectic A phase to the isotropic liquid, the correlation length collapses, as would be expected.

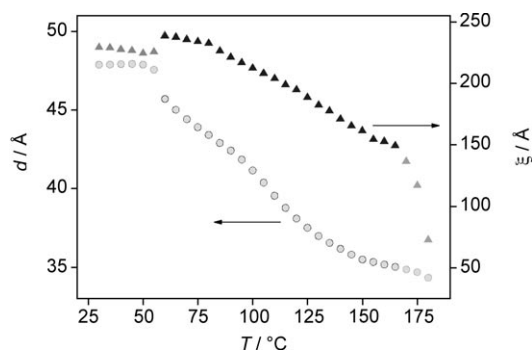


Figure 5. Temperature dependence of d_{001} and ξ_{001} for 6,6'-di-*O*-hexadecanoylsucrose, **2d**.

6,6'-*O*-Di-octadecanoylsucrose (**2e**): The diffraction intensity (using a logarithmic scale) as a function of the scattering wave vector q and temperature is shown in Figure 6 for

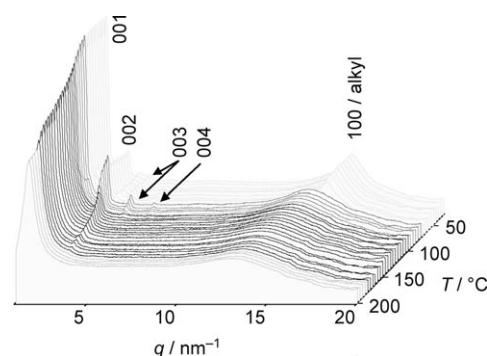


Figure 6. Radially integrated diffraction pattern of 6,6'-di-*O*-octadecanoylsucrose, **2e**, over a temperature range of 40–200 °C. Diffraction intensities are given on a logarithmic scale.

compound **2e**. Surprisingly, in contrast to the other materials studied, an intense small-angle reflection is observed in the isotropic phase, as shown by the light-grey curves in the figure, which indicates pretransitional effects occurring in the liquid. Upon cooling down into the smectic A phase (dark lines), the second-order reflection (002) can also be seen, which grows more intense as the temperature falls. At higher temperatures the fundamental (001) reflection is best fitted by a Lorentzian distribution function, taken from the peak width at half the peak height, indicating *short-range* positional order. At lower temperatures ($T < 100$ °C), the shape of the reflection changes to a Gaussian distribution function, indicating the presence of longer range positional order. Within this temperature range, third- and fourth-order reflections are also observed, indicating that the layers become better defined. The change in shape of the diffraction patterns for the fundamental reflections at $T = 105$ °C (Lorentzian) and $T = 95$ °C (Gaussian) are illustrated together in Figure 7. Note the difference in the shape of the curves, particularly at the “wings” of the reflections. Further cooling of the sample results in crystallization.

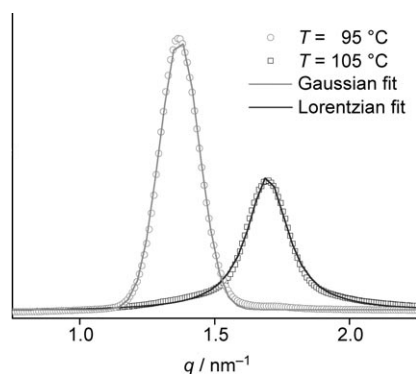


Figure 7. Lorentzian and Gaussian fits to the diffraction data at temperatures of 105 and 95°C, respectively, for compound **2e**.

A strong temperature dependence of the layer spacing is also observed in the smectic phase, with the d values ranging

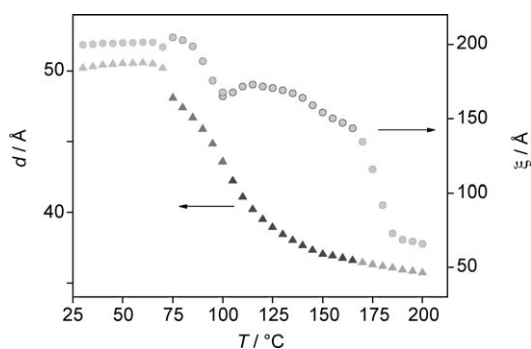


Figure 8. Temperature dependence of d_{001} and ξ_{001} for 6,6'-di-*O*-octadecanoylsucrose, **2e**.

from 35 to 50 Å; see Figure 8. Remarkably, the d spacing changes continuously in the smectic phase and into the isotropic liquid. Crystallization is observed between 70 and 75°C, at which d_{001} and ξ_{001} become virtually temperature independent. As the peak shape changes from Gaussian to Lorentzian ($T=100^\circ\text{C}$), a local minimum in the correlation length (half-width of the reflection) is observed, which marks a change in the form/structure of the smectic A phase. Table 5 shows a “snap-shot” of the d spacings taken at two temperatures, above and below this change. The

Table 5. X-ray data taken at two different temperatures in the smectic A phase of 6,6'-di-*O*-octadecanoylsucrose, **2e**.

T [°C]	Miller index	q [nm ⁻¹]	d [Å]	Ratio
80	001	1.32	47.4	1
	002	2.64	23.8	1/2
	003	3.98	15.8	1/3
	004	5.27	11.9	1/4
110	001	1.53	41.1	1
	002	3.04	20.7	1/2

fourth-order reflection at 80°C shows that the layers in the smectic phase are well defined.

At low temperatures the layer spacing approaches 48 Å, molecular modeling using ChemDraw 3D Ultra gives the length of the minimized, extended molecular conformation of 54.8 Å, and Dreiding Molecular Models give a value of 56 Å. At high temperatures the layer spacing approaches 36 Å, whereas modeling of the folded molecular conformation gives a value of 31.6 Å, and Dreiding Models a value of 29.7 Å. Figure 9 shows the ChemDraw-modeled fully extended and folded structures.

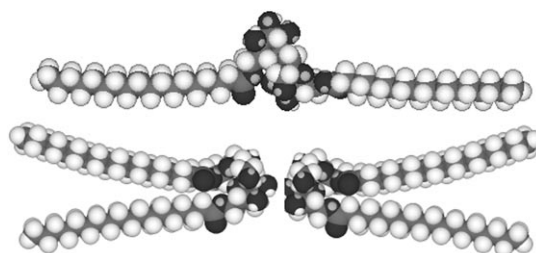


Figure 9. The fully extended structure (top), and the folded structure (bottom) for 6,6'-di-*O*-octadecanoylsucrose, **2e** (oxygen dark-grey, carbon mid-grey, hydrogen white).

One explanation for the transition in the smectic A phase is that the molecules are interdigitated at high temperature, and the extent of the interdigitation reduces as the temperature decreases as the phase becomes more ordered (Figure 10, top). Thus, it appears from the d -spacing measurements that there is a continuous transformation from an intercalated SmA_c to a nonintercalated SmA_1 ^[54] structuring of the layers. The transformation from the intercalated to the nonintercalated may be related to the change from Gaussian to Lorentzian line shape associated with the correlation length.

An alternative explanation could be that molecules have folded conformations, and at high temperatures the folded molecules pack in interdigitated bilayers, that is, as in the SmA_d phase.^[55,56] As the temperature is lowered the interdigitation is reduced and eventually the phase has only weak interdigitation, as in the SmA_2 phase^[54,55] (Figure 10, bottom). The changeover from one form of smectic A phase to the other may not be detected from the X-ray layer spacings, but it is possible that such a transition might be seen through examination of the correlation length.

The change in the correlation length is also associated with an increase in the number of reflections seen in the radial scans. At high temperatures only the first- and second-order reflections are seen, whereas at low temperatures the number of reflections increases to the fourth reflection. This suggests that the layers are becoming better defined at lower temperatures in the smectic A phase. The increased layer definition may be a result of the sugar units packing more strongly together due to extensive hydrogen-bonding interactions. The second model is probably more

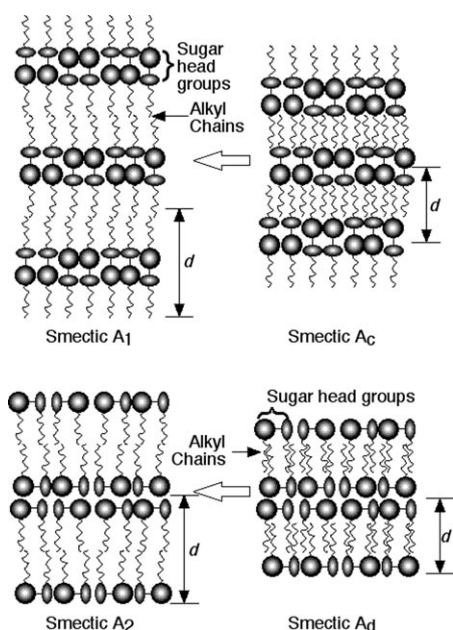


Figure 10. The intercalated to nonintercalated transformation for the fully extended molecular model (top), and the interdigitated to noninterdigitated transformation for the folded molecular model (bottom) for **2e**. For each drawing the left-hand side represents the lower-temperature structure.

likely than the first model to give well-defined layers described above. This is because the second arrangement allows for flexible interactions both between and within the layers, whereas the interlayer ordering for the first model has a greater dependency on the interfacial interactions between the aliphatic chains.

Whichever model is applied, such a substantial change in the layer spacing in a smectic A phase as a function of temperature has not yet been observed in conventional thermotropic liquid crystals, and smectic A polymorphism has not yet been observed in sugar-based mesogens.

Materials with mixed chain lengths

1'-O-Dodecanoyl-6'-O-hexadecanoylsucrose (1b): Figure 11 presents the diffraction intensity as a function of q and the temperature for the mixed chain-length compound **1b**, and the diffraction data taken at 50 °C are summarized in Table 6.

The temperature dependence of the layer spacing d_{001} and the correlation length ξ_{001} are shown in Figure 12. The evolution of ξ_{001} clearly indicates a phase transition between 110–120 °C, as observed by DSC and POM (value = 115.9 °C). The layer spacing shows a continuous increase as temperature decreases, and over a temperature range of 80 °C it increases by 6 Å, an increase of approximately 17%. Interestingly, the correlation length changes rapidly at the transition to the liquid, however, the layer ordering is relatively continuous over 15 °C above the phase transition. These results suggest that there is some persistence of the

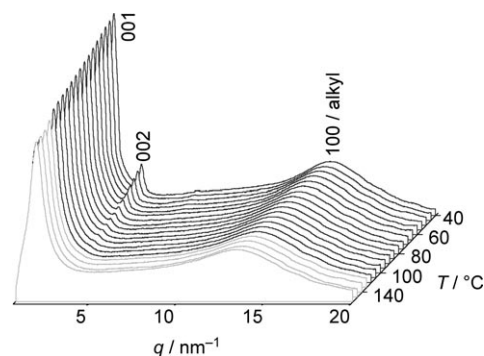


Figure 11. Radially integrated diffraction pattern of 1'-O-dodecanoyl-6'-O-hexadecanoylsucrose, **1b**, over a temperature range of 30–160 °C. Diffraction intensities are given on a logarithmic scale. The light-grey lines are within the liquid state and the dark lines are within the smectic A phase.

Table 6. Distances (d) related to the Miller indices for the radially integrated diffraction pattern of 1'-O-dodecanoyl-6'-O-hexadecanoylsucrose, **1b**, at 50 °C.

Miller index	q [nm ⁻¹]	d [Å]	Ratio
001	1.64	38.6	1
002	3.26	19.3	–
alkyl/100	13.8	4.5	–

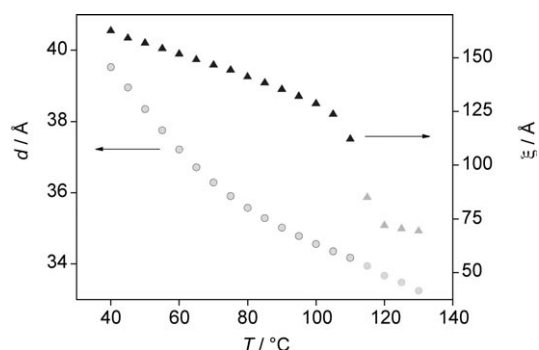


Figure 12. Temperature dependence of d_{001} and ξ_{001} for 1'-O-dodecanoyl-6'-O-hexadecanoylsucrose, **1b**.

layer ordering into the liquid phase, hence, the liquid could be said to be structured.

Mixture of 6,6'-di-O-dodecanoyl-hexadecanoylsucroses (3a): Figure 13 presents the diffraction intensity as a function of q and temperature for the mixed system **3a**. The diffraction data taken at a temperature of 50 °C are summarized in Table 7. A small (002) reflection is visible from 145 °C onwards, and even a 004 reflection is obtained at low temperatures, indicating that the layers are well defined in the smectic A phase. However, the 003 reflection appears to be very weak and almost nonexistent. The clearing-point transition obtained between 155 and 160 °C, rather than the expected 167.8 °C, is clearly visible from the change in shape of the

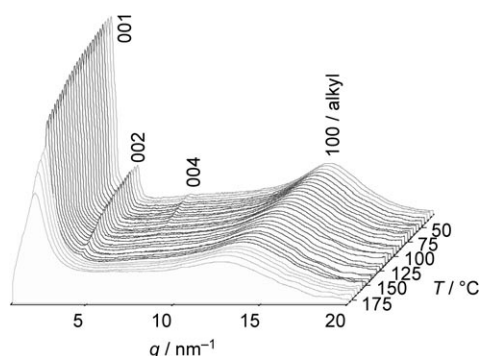


Figure 13. Radially integrated diffraction pattern of the mixture of 6,6'-dodecanoyl-hexadecanoylsucroses, **3a**, over a temperature range of 40–180 °C.

Table 7. Distances (d) related to the Miller indices for the radially integrated diffraction pattern for the mixture of 6,6'-dodecanoyl-hexadecanoylsucroses, **3a**, at 50 °C.

Miller index	q [nm^{-1}]	d [\AA]	Ratio
001	1.55	40.5	1
002	3.11	20.2	–
004	6.21	11.2	–
alkyl/001	13.9	4.5	–

reflection. This change in clearing point is possible due to slight decomposition of the sample.

Figure 14 shows the temperature dependence of the layer spacing, d_{001} , and the correlation length, ξ_{001} . A strong dependence of the layer spacing is observed throughout the

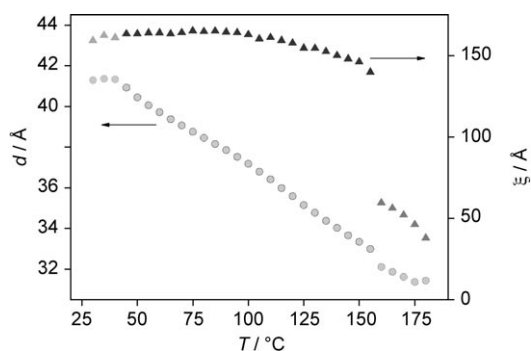


Figure 14. Temperature dependence of d_{001} and ξ_{001} for the mixture of 6,6'-dodecanoyl-hexadecanoylsucroses, **3a**.

temperature range of the smectic A phase. However, a small discontinuity in the layer spacing is observed at the transition from the liquid-crystal phase to the liquid, thus, the liquid of **3a** appears to be structured. A much greater discontinuity at the isotropization point is seen for the correlation length; conversely, in the crystalline state the layer spacing and the correlation length are nearly constant.

A comparison of the layer spacings as a function of temperature for the materials **1b**, **2a**, **2d**, **2e**, and **3a** is given in

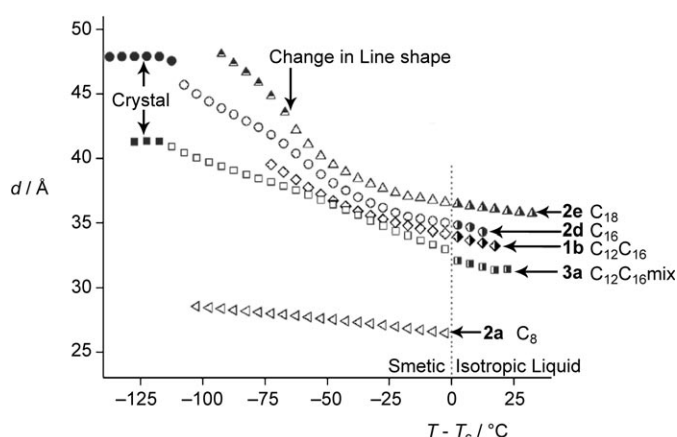


Figure 15. Evolution of the layer spacing d (\AA) as a function of the reduced temperature for the smectic A phases of the diesters **1b**, **2a**, **2d**, **2e**, and **3a**. T_c is the normalized clearing point for each material.

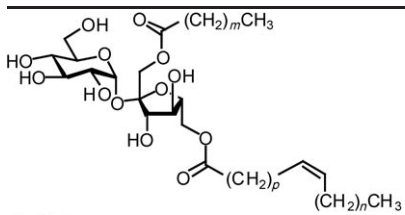
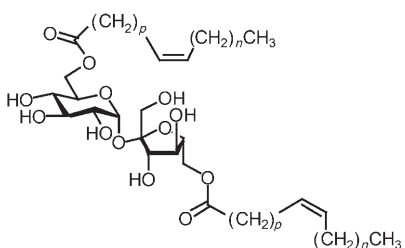
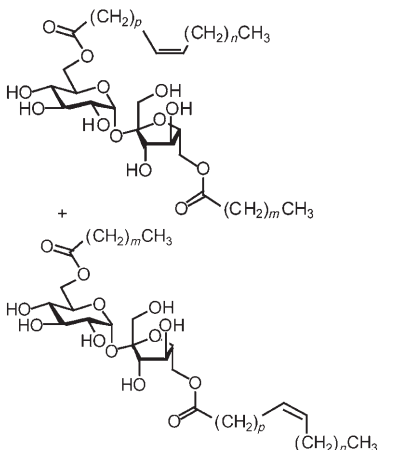
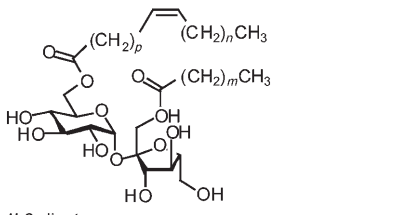
Figure 15. This figure clearly demonstrates, for the materials with shorter aliphatic chains, that the layer spacing is relatively independent of temperature, whereas the longer chain lengths show very large temperature dependencies. Moreover, the temperature dependency increases as aliphatic chain length increases (compare **2a** (C8), **2d** (C16), and **2e** (C18)). In addition, for the longer chains the layer ordering persists well into the liquid phase. Furthermore, comparison of **1b**, which has a defined substitution pattern, with the mixed system **3a** reveals a very similar temperature dependency of the layer spacing. However, the mixed system has a much wider temperature range, possibly due to the disordering introduced by having mixed systems.

2. Unsaturated fatty-acid diesters

Polarizing light microscopy: Glycolipids found in nature often possess *cis* unsaturations in their aliphatic chains. Thus, to complement the study of the liquid-crystalline-saturated sucrose esters, a selection of unsaturated analogues were prepared. Table 8 summarizes the observations obtained by microscopy of the phase transitions for homogeneous or mixed diesters with one or two chains being monounsaturated. The first observation to be made from the transition temperatures is that the unsaturated aliphatic materials possess soft-crystal phases for which the phase transitions to the liquid-crystalline state could not be determined by microscopy, and no definitive enthalpies could be observed for the transitions by DSC.

Secondly, unlike the saturated materials, at long chain lengths columnar phases replaced lamellar phases. For example, compounds **1d** and **2h**, in which the total number of carbon atoms in the chains ≥ 14 , exhibited columnar phases, whereas the shorter homologues **1c**, **2f**, **2g**, **3b**, and **4a** exhibit smectic A phases. Compound **2g** (6,6'-substitution and two unsaturations) demonstrates that there is still some effect of the positions of attachment of the chains and level of unsaturation, as this material exhibits a smectic phase. In

Table 8. Transition temperatures determined by optical microscopy for the unsaturated fatty-acid sucrose diesters.

Sucrose diester	Chain length	Compd	Transition temperature [°C]
	$m=10, n=5, p=3$	1c	soft solid–smectic A 110 iso. liq.
	$m=14, n=5, p=7$	1d	soft solid–col. 121 iso. liq.
1',6'-diesters			
	$n=5, p=3$	2f	soft solid–smectic A 138.5 iso. liq.
	$n=5, p=7$	2g	soft solid–smectic A 144.6 iso. liq.
	$n=7, p=7$	2h	soft solid–col. 146.3 iso. liq.
6,6'-diesters			
	$m=10, n=5, p=3$	3b	soft solid–smectic A 158.8 iso. liq.
mixture of-6,6'-diesters			
	$m=10, n=5, p=3$	4a	soft solid–smectic A 128.5 iso. liq.
1',6'-diester			

contrast, compound **1d**, which has the same number of carbon atoms in the chains (1',6'-substitution and one unsaturation) possesses a columnar phase. The type of columnar phases present appeared to be disordered hexagonal phases, suggesting that the unsaturated aliphatic chain cross-sectional areas were expanded relative to those of the saturated chains, thereby causing the introduction of curvature into the self-organization. Therefore, the structure of the columns is disordered with respect to the positions of the molecules and their up and down orientations.

Figure 16 shows the defect texture of the columnar phase of compound **2h**. The texture is characterized by the absence of homeotropic alignment and the lack of hyperbolic and elliptical lines of optical discontinuity. However, the fanlike regions are classical signatures for the presence of a columnar phase.

Differential scanning calorimetry (DSC): To aid comparison, the DSC data for the clearing-point enthalpies and entropies of the esters **2f**, **2g**, **2h**, **3b**, and **4a** are listed in Table 9. By comparing these results with those in Table 2, it is clear that the presence of a *cis* double bond in the aliphatic chains induces a decrease in the relative isotropization temperature. Similarly, the enthalpy and entropy values are slightly lower, indicating that the unsaturated systems form more-disordered liquid-crystal phases than their saturated analogues. In addition, the enthalpy and entropy values for the columnar to the isotropic liquid-crystal phase transition for **2h** are almost one order of magnitude lower than those for the lamellar phase to the isotropic liquid transition for compounds **2f**, **2g**, and **3b**. This result indicates that the structure within the columnar phases is disordered and liquid-like, and even the columns themselves may not be periodically ordered on a hexagonal lattice. Furthermore, the low enthalpy and entropy values indicate the structuring in the liquid-crystal state is similar to

that in the liquid, and, thus, the liquid itself is structured. Conversely, compound **4a** appears to have intermediary values between the lamellar and the columnar materials, indicating that this compound may be located at the crossover in the phase behavior.

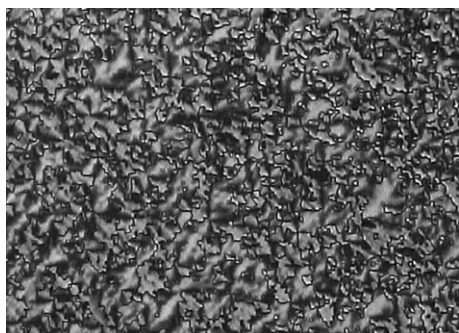


Figure 16. Defect texture (x100) of the columnar mesophase of 6,6'-di-O-oleoylsucrose, **2h**.

Table 9. Clearing-point temperatures, clearing-point enthalpies, ΔH , and clearing-point entropies, ΔS , for the unsaturated fatty-acid diesters **2f**, **2g**, **2h**, **3b**, and **4a**.

Compound	Clearing point [°C]	ΔH [J g ⁻¹]	ΔS [mJ g ⁻¹ K ⁻¹]
2f		2.645	6.43
2g		1.386	3.32
2h		0.122	0.29
3b	158.8	2.971	6.88
4a	128.5	0.847	2.11

Conclusion

We have shown that the position of substitution on the sucrose scaffold affects the mesophase stability, and the 1',6'-diesters have lower mesophase stabilities than the 6,6'-diesters. If long unsaturated chains are appended to the scaffold, columnar phases can occur, which is probably related to the larger effective cross-sectional areas of the chains. In addition, we have demonstrated for sucrose diesters that there can be very large changes in the layer spacings in smectic A phases as a function of temperature. If such changes occur, it is possible to have abrupt changes in the correlation lengths, leading to an unusual and novel phase behavior in the lamellar phase. Layer ordering and the correlation length in lamellar phases can extend into the liquid phase, which indicates that the liquid itself is structured/ordered. The inclusion of *cis* unsaturated aliphatic chains, rather than fully saturated chains, leads to the formation of columnar phases in preference to lamellar phases. These results may have some relevance to biological systems, and to membranes in particular.

Acknowledgements

This work was achieved partly in the former Béghin-Say-CNRS research facility in Villeurbanne (CNRS UMR 143). Financial support from these institutions, and a grant from ANRT to V.M., are gratefully acknowledged.

[1] D. M. Small, *J. Colloid Interface Sci.* **1977**, *58*, 581–602.

- [2] R. Koyanova, M. Caffrey, *Biochim. Biophys. Acta* **1995**, *1255*, 213–236.
- [3] E. Fischer, B. Helferich, *Justus Liebigs Ann. Chem.* **1911**, *383*, 68–70; D. C. Carter, J. R. Ruble, G. A. Jeffrey, *Carbohydr. Res.* **1982**, *102*, 59–67; G. A. Jeffrey, S. Bhattacharjee, *Carbohydr. Res.* **1983**, *115*, 53–58; J. W. Goodby, *Mol. Cryst. Liq. Cryst.* **1984**, *110*, 205–219; G. A. Jeffrey, *Mol. Cryst. Liq. Cryst.* **1984**, *110*, 221–237; B. Pfannemüller, W. Welte, E. Chin, J. W. Goodby, *Liq. Cryst.* **1986**, *1*, 357–370; D. Blunk, K. Praefcke, V. Vill in *Handbook of Liquid Crystals Vol. 3: High Molecular Weight Liquid Crystals* (Eds.: D. Demus, J. W. Goodby, G. W. Gray, H.-W. Spiess, V. Vill), Wiley-VCH, Weinheim, **1998**, pp. 305–340, and references therein.
- [4] Y. Queneau, J. Gagnaire, J. J. West, G. Mackenzie, J. W. Goodby, *J. Mater. Chem.* **2001**, *11*, 2839–2844.
- [5] K. Hill, O. Rhode, *Fett/Lipid* **1999**, *101*, 25–33.
- [6] I. J. A. Baker, B. Matthews, H. Soares, I. Krodkiwska, D. N. Furlong, F. Grieser, C. J. Drummond, *J. Surfactants Deterg.* **2000**, *3*, 1–11.
- [7] S. Nakamura, *INFORM* **1997**, *8*, 866–874.
- [8] P. Simon, S. Veyrat, P. Piquemal, C. Montastier, V. Goffin, G. E. Pierard, *Cosmet. Toiletries* **1998**, *113*, 69–72.
- [9] A. Guerrero, P. Partal, C. Gallegos, *J. Rheol.* **1998**, *42*, 1375–1388.
- [10] A.-S. Muller, J. Gagnaire, Y. Queneau, M. Karaoglanian, J.-P. Maitre, A. Bouchu, *Colloids Surf. A* **2002**, *203*, 55–66.
- [11] N. Garti, V. Clement, M. Leser, A. Aserin, M. Fanun, *J. Mol. Liq.* **1999**, *80*, 253–296.
- [12] M. A. Bolzinger-Thevenin, J. L. Grossiord, M. C. Poelman, *Langmuir* **1999**, *15*, 2307–2315.
- [13] M. H. Kabir, M. Ishitobi, H. Kunieda, *Colloid Polym. Sci.* **2002**, *280*, 841–847.
- [14] S. E. Ebeler, L. M. Breyer, C. E. Walker, *J. Food Sci.* **1986**, *51*, 1276–1279.
- [15] C. J. Drummond, C. Fong, I. Krodkiwska, B. J. Boyd, I. J. A. Baker in *Novel Surfactants: Preparation, Applications, and Biodegradability*, 2nd ed. (Ed.: K. Holmberg), Marcel Dekker, New York, **2003**, pp. 95–128.
- [16] B. A. P. Nelen, J. M. Cooper in *Emulsifiers in Food Technology* (Ed.: R. J. Whitehurst), Blackwell, Oxford, **2004**, pp. 131–161.
- [17] M. Ferrer, F. Comelles, F. J. Plou, M. A. Cruces, G. Fuentes, J. L. Parra, A. Ballesteros, *Langmuir* **2002**, *18*, 667–673.
- [18] G. Garofalakis, B. S. Murray, *Langmuir* **2002**, *18*, 4764–4774.
- [19] G. Garofalakis, B. S. Murray, D. B. Sarney, *J. Colloid Interface Sci.* **2000**, *229*, 391–398.
- [20] I. Söderberg, C. J. Drummond, D. N. Furlong, S. Godkin, B. Matthews, *Colloids Surf. A* **1995**, *102*, 91–97.
- [21] T. Kawaguchi, T. Hamanaka, Y. Kito, H. Machida, *J. Phys. Chem.* **1991**, *95*, 3837–3846.
- [22] Y. Li, S. Zhang, J. Yang, Q. Wang, *Colloids Surf. A* **2004**, *248*, 127–133.
- [23] Y. Li, S. Zhang, Q. Wang, J. Yang, *Tenside, Surfactants, Deterg.* **2004**, *41*, 26–30.
- [24] V. Molinier, B. Fenet, J. Fitremann, A. Bouchu, Y. Queneau, *J. Colloid Interface Sci.* **2005**, *286*, 360–368.
- [25] T. Rades, C. C. Müller-Goymann, *Colloid Polym. Sci.* **1997**, *275*, 1169–1178.
- [26] V. Sadtler, M. Guely P. Marchal, L. Choplin, *J. Colloid Interface Sci.* **2004**, *270*, 270–275.
- [27] V. Molinier, P. J. J. Kouwer, J. Fitremann, A. Bouchu, G. Mackenzie, Y. Queneau, J. W. Goodby, *Chem. Eur. J.* **2006**, *12*, 3547–3557.
- [28] C. M. Paleos, D. Tsiourvas, *Curr. Opin. Colloid Interface Sci.* **2001**, *6*, 257–267.
- [29] G. Milkereit, M. Morr, J. Thiem, V. Vill, *Chem. Phys. Lipids* **2004**, *127*, 47–63.
- [30] H. Van Doren, E. Smits, M. Pestman, J. B. F. N. Engberts, R. M. Kellogg, *Chem. Soc. Rev.* **2000**, *29*, 183–199.
- [31] R. Auzely-Velty, T. Benvegnu, G. Mackenzie, J. A. Haley, J. W. Goodby, D. Plusquellec, *Carbohydr. Res.* **1998**, *314*, 65–77.
- [32] F. Dumoulin, D. Lafont, P. Boullanger, G. Mackenzie, G. H. Mehl, J. W. Goodby, *J. Am. Chem. Soc.* **2002**, *124*, 13737–13748.

- [33] C. E. Fairhurst, S. Fuller, J. Gray, M. C. Holmes, G. J. T. Tiddy in *Handbook of Liquid Crystals Vol. 3: High Molecular Weight Liquid Crystals* (Eds.: D. Demus, J. W. Goodby, G. W. Gray, H.-W. Spiess, V. Vill), Wiley-VCH, Weinheim, **1998**, pp. 341–392, and references therein.
- [34] B. J. Boyd, C. J. Drummond, I. Krodziewska, F. Grieser, *Langmuir* **2000**, *16*, 7359–7367.
- [35] V. Vill, T. Böcker, J. Thiem, F. Fisher, *Liq. Cryst.* **1989**, *6*, 349–356.
- [36] B. Hoffmann, G. Platz, *Curr. Opin. Colloid Interface Sci.* **2001**, *6*, 171–177.
- [37] H. M. Von Minden, K. Brandenburg, U. Seydel, M. H. J. Koch, V. Garamus, R. Willumeit, V. Vill, *Chem. Phys. Lipids* **2000**, *106*, 157–179.
- [38] P. Boullanger, *Top. Curr. Chem.* **1997**, *187*, 275–312.
- [39] V. Vill, R. Hashim, *Curr. Opin. Colloid Interface Sci.* **2002**, *7*, 395–409.
- [40] S. Bottle, I. D. Jenkins, *J. Chem. Soc. Chem. Commun.* **1984**, 385.
- [41] I. D. Jenkins, M. B. Goren, *Chem. Phys. Lipids* **1986**, *41*, 225–235.
- [42] V. Molinier, P. H. J. Kouwer, Y. Queneau, J. Fitremann, G. Mackenzie, J. W. Goodby, *Chem. Commun.* **2003**, 2860–2861.
- [43] Y. Queneau, J. Fitremann, S. Trombotto, *C. R. Chim.* **2004**, *7*, 177–188.
- [44] V. Molinier, J. Fitremann, A. Bouchu, Y. Queneau, *Tetrahedron: Asymmetry* **2004**, *15*, 1753–1762.
- [45] V. Molinier, K. Wisniewski, A. Bouchu, J. Fitremann, Y. Queneau, *J. Carbohydr. Chem.* **2003**, *22*, 657–669.
- [46] S. Thévenet, A. Wernicke, S. Belniak, G. Descotes, A. Bouchu, Y. Queneau, *Carbohydr. Res.* **1999**, *318*, 52–66.
- [47] P. Potier, A. Bouchu, G. Descotes, Y. Queneau, *Synthesis* **2001**, 458–462.
- [48] S. Riva, J. Chopineau, A. P. G. Kieboom, A. M. , Klibanov, *J. Am. Chem. Soc.* **1988**, *110*, 584–589.
- [49] G. Carrea, S. Riva, F. Secundo, B. Danieli, *J. Chem. Soc. Perkin Trans. 1* **1989**, 1057–1061.
- [50] P. Potier, A. Bouchu, G. Descotes, Y. Queneau, *Tetrahedron Lett.* **2000**, *41*, 3597–3600.
- [51] T. Polat, H. G. Bazin, R. J. Linhardt, *J. Carbohydr. Chem.* **1997**, *16*, 1319–1325.
- [52] P. Potier, A. Bouchu, J. Gagnaire, Y. Queneau, *Tetrahedron: Asymmetry* **2001**, *12*, 2409–2419.
- [53] *CRC Handbook of Physics and Chemistry*, 68th ed. (Ed.: R. C. Priest), CRC Press, Boca Raton, **1988**.
- [54] C. T. Imrie, G. R. Luckhurst in *Handbook of Liquid Crystals Vol. 2b: High Molecular Weight Liquid Crystals* (Eds.: D. Demus, J. W. Goodby, G. W. Gray, H.-W. Spiess, V. Vill), Wiley-VCH, Weinheim, **1998**, pp. 801–833, and references therein.
- [55] F. Hardouin, A.-M. Levelut, J. J. Benatter, G. Sigaud, *Solid State Commun.* **1980**, *33*, 337–340.
- [56] F. Hardouin, G. Sigaud, N. H. Tinh, M. F. Achard, *J. Phys. Lett.* **1981**, *42*, 63–66.

Received: March 15, 2006

Revised: July 10, 2006

Published online: November 23, 2006